Biochimica et Biophysica Acta 1848 (2015) 1111–1118

Contents lists available at ScienceDirect

Biochimica et Biophysica Acta

journal homepage: www.elsevier.com/locate/bbamem

The role of C-terminal amidation in the membrane interactions of the anionic antimicrobial peptide, maximin H5

Sarah R. Dennison [a,b], Manuela Mura [c], Frederick Harris [b,d], Leslie H.G. Morton [d], Andrei Zvelindovsky [e], David A. Phoenix [b,d,*]

[a] School of Pharmacy and Biomedical Sciences, University of Central Lancashire, Preston PR1 2HE, UK
[b] School of Applied Science, London South Bank University, 103 Borough Road, London SE1 0AA, UK
[c] School of Computing Engineering and Physical Science, University of Central Lancashire, Preston PR1 2HE, UK
[d] School of Forensic and Investigative Science, University of Central Lancashire, Preston PR1 2HE, UK
[e] School of Mathematics and Physics, University of Lincoln, Lincolnshire LN6 7TS, UK

ARTICLE INFO

Article history:
Received 22 September 2014
Received in revised form 2 January 2015
Accepted 21 January 2015
Available online 30 January 2015

Keywords:
Anionic antimicrobial peptide
α-Helical
Haemolysis
Lipid monolayer
Lysis

ABSTRACT

Maximin H5 is an anionic antimicrobial peptide from amphibians, which carries a C-terminal amide moiety, and was found to be moderately haemolytic (20%). The α-helicity of the peptide was 42% in the presence of lipid mimics of erythrocyte membranes and was found able to penetrate (10.8 mN m^{-1}) and lyse these model membranes (64 %). In contrast, the deaminated peptide exhibited lower levels of haemolysis (12%) and α-helicity (16%) along with a reduced ability to penetrate (7.8 mN m^{-1}) and lyse (55%) lipid mimics of erythrocyte membranes. Taken with molecular dynamic simulations and theoretical analysis, these data suggest that native maximin H5 primarily exerts its haemolytic action via the formation of an oblique orientated α-helical structure and tilted membrane insertion. However, the C-terminal deamination of maximin H5 induces a loss of tilted α-helical structure, which abolishes the ability of the peptide's N-terminal and C-terminal regions to H-bond and leads to a loss in haemolytic ability. Taken in combination, these observations strongly suggest that the C-terminal amide moiety carried by maximin H5 is required to stabilise the adoption of membrane interactive tilted structure by the peptide. Consistent with previous reports, these data show that the efficacy of interaction and specificity of maximin H5 for membranes can be attenuated by sequence modification and may assist in the development of variants of the peptide with the potential to serve as anti-infectives.

1. Introduction

Antimicrobial peptides (AMPs) are ancient components of the innate immune systems that are found in creatures from across the eukaryotic kingdom and they possess potent activity against a wide spectrum of bacteria, viruses, fungi and parasites [1,2]. In general, this activity involves membrane interaction [3,4] and increasingly, it has been found that post-translational modifications (PTMs) play a role in optimising the efficacy and specificity of these mechanisms of action [5–9]. Most of the PTMs identified in AMPs are relatively infrequent in occurrence [6], typically the phosphorylation of residues [1,6,10] and the chiral inversion of residues to produce D-amino acids [11–13]. However, two PTMs have been found to be ubiquitous amongst AMPs of eukaryotes [6] of which the first is the oxidation of cysteine residues to form disulphide bridges [14]. It is generally accepted that disulphide bridges play a major architectural role in the antimicrobial action of AMPs [6], primarily by maintaining the amphiphilic topography of the molecules and thereby their ability to interact with target membranes and kill host cells [5,15]. This form of structural stabilisation is also important for the therapeutic development of AMPs as seen with the cysteine knot architectures of cyclotides from plants [2,16]. The exceptional stability of these peptides coupled to their high tolerance of residue substitutions [17] makes them potential candidates to serve as lead compounds in scenarios ranging from tumour imaging [18] to preventing the sexual transmission of HIV [19].

The second most common PTM found in AMPs is the introduction of C-terminal moieties, which have predominantly been identified in amphibians [6]. These fall into two major classes: the presence of either a Rana box [20] or an amide group [21]. The Rana box is found in the vast majority of Ranid frogs and consists of a C-terminal cyclic heptapeptide with a conserved disulphide bond [20,22,23]. This PTM occurs in AMPs such as gaegurins and palustrins and appears to play a role in facilitating the membrane affinity of these peptides by stabilising their C-terminal structure [20,24]. In contrast, the importance of C-terminal amidation in the antimicrobial action of amphibian and other AMPs is far from

Abbreviations: α-AMPs, α-helical antimicrobial peptides; CD, circular dichroism; DMPC, dimyristoylphosphatidylcholine; MD, molecular dynamic; PTMs, post-translational modifications

* Corresponding author at: London South Bank University, 103 Borough Road, London SE1 0AA, UK. Tel.: +44 20 7815 6001; fax: +44 20 7815 6099.
E-mail address: phoenixd@lsbu.ac.uk (D.A. Phoenix).

http://dx.doi.org/10.1016/j.bbamem.2015.01.014
0005-2736/

clearly understood [25]. Most recently, a suite of homologous AMPs, maximin H1 to maximin H55, were identified in toads from the *Bombina* genus. These AMPs all exhibited C-terminal amidation, clearly suggesting functional relevance [26–28]. Studies on synthetic AMPs have shown that C-terminal amidation can enhance antibacterial efficacy without increasing lytic ability thereby increasing the therapeutic potential of these peptides [29]. Given that maximin H5 from *Bombina maxima* has potent, narrow range, antibacterial activity [30], we have investigated the role of C-terminal amidation in the interactions of the peptide with erythrocyte membranes to help elucidate the suitability of the peptide for medical use.

2. Materials and methods

2.1. Reagents

A synthetic homologue of maximin H5, MH5N (ILGPVLGLVSD TLDDVLGIL-$CONH_2$), and its C-terminally deamidated isoform, MH5C (ILGPVLGLVSDTLDDVLGIL-COOH), were manufactured by Pepceuticals (Leicestershire, UK) by solid state synthesis and purified by HPLC to purity greater than 95%. Dimyristoyl phosphatidylcholine (DMPC) was supplied by Avanti Polar Lipids (Alabaster, Alabama) and used without further purification and analysed using mass spectrometry (Fig. S1). All other reagents were supplied by SIGMA (UK) and VWR (UK) unless otherwise stated.

2.2. The antibacterial assay of maximin H5 isoforms

Cultures of *Escherichia coli*, strain W3110, and *Staphylococcus aureus*, strain UL12, which had both been freeze-dried in 20% (v/v) glycerol and stored at −80 °C, were used to inoculate 10 ml aliquots of sterile nutrient broth and incubated at 37 °C until the exponential phase was reached (OD = 0.6; λ = 600 nm). The cell cultures were then centrifuged at 15,000 ×*g* at 4 °C for 15 min using a bench top centrifuge. The resulting pellet was washed three times in 25% strength Ringer's solution and then re-suspended in 1 ml Ringer's solution. 1 ml aliquots of maximin H5 isoforms ranging from 0 μM to 1000 μM were prepared separately in 25% strength Ringer's solution by the double dilution method. 20 μl of each test bacterial suspension was added to separate 1 ml aliquots of peptide and incubated at 37 °C for 48 h. After incubation, each bacterial culture was streaked onto nutrient agar plates so as to create a six-spoked star wheel and incubated at 37 °C for 12 h as previously described by Dennison et al. [31]. This method was carried out in triplicate. The minimum inhibition concentration (MIC) was determined from the lowest final concentration of peptide at which no growth was observed during the predetermined period of incubation in any of the triplicate samples.

2.3. The haemolytic ability of maximin H5 isoforms

The haemolytic activity of MH5N and MH5C were investigated using fresh human red blood cells (3 ml), which were washed 3 times with phosphate buffered saline (PBS, pH 7.4) by centrifugation for 5 min at 1200 ×*g* until the supernatant was clear. Washed red blood cells were resuspended in PBS to a final volume of 20 ml. Peptide solutions (10 μl) were added to a 190 μl suspension of washed red blood cells and incubated for 1 h at 37 °C. The samples were then centrifuged at 12,000 ×*g* for 5 min. The release of haemoglobin was monitored by diluting 100 μl of supernatant with 900 μl PBS and measuring the absorbance at 576 nm [$A_{Peptide}$]. For negative and positive controls, PBS buffer [A_{PBS}] and 0.1% Triton X-100 [A_{Triton}] were used. These experiments were performed in quadruplicate and the mean percentage haemolysis calculated using the equation [32,33]:

$$Pecentage\,haemolysis = \frac{\left[A_{Peptide}\right] - [A_{PBS}]}{[A_{Triton}] - [A_{PBS}]} \times 100.$$

2.4. Secondary structural analysis of maximin H5 isoforms

Secondary structure analysis of MH5N and MH5C was performed using a J-815 spectropolarimeter (Jasco, UK) at 20 °C, as previously described [34]. Samples were prepared by dissolving the peptides in phosphate buffered saline (PBS) and 2,2,2-trifluoroethanol/phosphate buffered saline (TFE/PBS; 50% v/v) to give a final peptide concentration of 60 μM in each case. Circular dichroism (CD) structural analysis was also performed with MH5N and MH5C in the presence of lipid. DMPC (19 mg ml^{-1}) was dissolved in chloroform, dried under N_2 gas before being vacuum-dried, and the resulting lipid film rehydrated using 1 × PBS (pH 7.5) for an hour, or until the solution was no longer turbid. These samples were then freeze-thawed 4 times, followed by extrusion 11 times with a 0.1 μm polycarbonate filter using an Avanti Polar Lipids mini-extruder apparatus. Peptide/lipid samples were prepared by adding stock peptide solution to a measured volume of lipid suspension to obtain the desired peptide:lipid molar ratio (1:100) before being mixed thoroughly. Far UV (180 to 260 nm) CD spectra were recorded using 0.5 nm intervals, a bandwidth of 1 nm, a scan speed of 100 nm min^{-1} and a 10 mm path-length cell. Four scans per sample were performed and averaged. For secondary structure estimation, the CD spectra were deconvoluted using the CDSSTR algorithm (protein reference set 3) on the DichroWeb server [35–37].

2.5. Lipid monolayer analysis of maximin H5 isoforms

Lipid monolayers of DMPC were formed by dropping chloroformic solutions of the lipid onto a Tris buffer subphase (10 mM; pH 7.5) contained in an 80 ml 601 M Langmuir Teflon trough (Biolin Scientific/KSV NIMA, UK). Surface pressure (π) was measured using a Wilhelmy wire attached to a microbalance. After spreading, the solvent was allowed to evaporate off the subphase surface over 30 min and the barriers were closed at a rate of 5 cm^2 min^{-1} until a starting pressure of 30 mN m^{-1} was achieved, which is equivalent to that of the outer leaflet of a cell membrane [38]. Monolayers were allowed to equilibrate for a further 30 min before MH5N and MH5C were injected into the subphase using an L-shaped Hamilton syringe without disruption of the monolayer.

2.6. The lytic ability of maximin H5 isoforms

DMPC (7.5 mg) was dissolved in chloroform and dried under N_2 gas before being vacuum-dried. The resulting lipid film was then hydrated with 1 ml of HEPES (5.0 mM; pH 7.5) containing calcein (70 mM). The suspension was vortexed for 5 min and then sonicated for 30 min after which, the solution underwent 3 cycles of freeze-thawing. Liposomes were extruded 11 times through a 0.1 μm polycarbonate filter using an Avanti polar lipids mini-extruder apparatus. Calcein entrapped vesicles were separated from free calcein by gel filtration using a Sephadex G75 column (Sigma Aldrich, UK) which was rehydrated overnight in HEPES (20 mM; pH 7.5), NaCl (150 mM) and EDTA (1.0 mM). The column was then eluted with HEPES (5 mM; pH 7.5).

The calcein release assay was performed by combining 2 ml of HEPES (20 mM; pH 7.5), NaCl (150 mM) and EDTA (1.0 mM) with 20 μl of calcein vesicles. MH5N and MH5C (90 μM) were incubated with these vesicles and the fluorescence intensities of released calcein measured using an FP-6500 spectrofluorometer (Jasco, UK), with an excitation wavelength of 490 nm and emission wavelength of 520 nm. Membrane lysis of 100% was taken as the fluorescence induced by

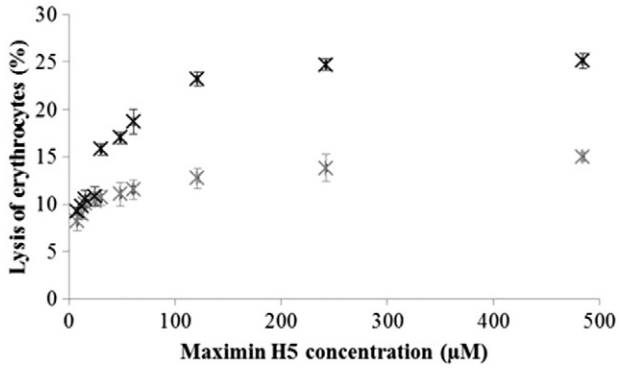

Fig. 1. The haemolytic ability of isoforms of maximin H5. The figure shows the haemolytic activity of MH5N (black) and MH5C (grey) towards human red blood cells. MH5N showed greater activity towards these cells than MH5C with these peptides inducing 20% and 12% lysis, respectively, at 90 μM, which is the reported antibacterial minimum inhibitory concentration (MIC) for maximin H5 [28,39]. These experiments were performed in quadruplicate and error bars represent the standard deviation.

Triton ×100 (20 μl) when used to dissolve the vesicles. The percentage lysis achieved by MH5N and MH5C was then calculated relative to this standard.

2.7. MD simulations of maximin H5 isoforms

The conformational behaviour and lipid interactivity of MH5N and MH5C in the presence of DMPC membranes was examined by molecular dynamics calculations, as previously described [39]. Using peptide/lipid ratios of 3:128, models for MH5N and MH5C were assembled as canonical α-helices using AMBER tools 12 as previously described [39]. Simulations and analysis were performed using GROMACS and the GROMOS96 53a6 force field was used with the step descended method. Bilayer parameters were used from references and the simple point-charge (SPC) water model was used in all simulations. All structures were equilibrated at room temperature in water in the sequence: minimization, NVT and NPT simulations. The simulations in water were performed by solvating the peptide in a box: 6 nm × 6 nm × 6 nm with approximately 8000 water molecules. Counter-ions (Na^+, Cl^-) were added to the system to make it neutral. The peptide was simulated with backbone atoms restrained in NVT and then NPT ensemble with pressure maintained at 1 atm by isotropic coupling to a Berendsen barostat and the temperature maintained at 303 K. A free molecular dynamic simulation of 200 ns without restraint was performed at constant temperature, pressure and number of molecules (NPT ensemble). The membrane was simulated using a DMPC bilayer containing 128 lipid molecules in a box 7 nm × 7 nm × 9.0 nm (xyz box) with the bilayer normal being parallel to the z-axis. An equilibration run was 400 ns long at 303 K in a box containing circa 10,000 water molecules. For both MH5N and MH5C, three peptide molecules were inserted into the box containing the solvated bilayer. An equilibration run of 2 ns was carried out for the peptide-bilayer system with the position of the peptides restrained using harmonic restrains with constant force of 1.0 kJ^{-1} nm^{-2} per atom. The cut off for both van der Waals and Coulombic interactions was 1.2 nm. Berendsen temperature coupling was used at 303 K and the water and the bilayer were coupled separately. A semi-isotropic Berendsen barometer was used. The main molecular dynamics simulation (no restraints) runs were performed at constant temperature, pressure and number of molecules.

3. Results

3.1. The antibacterial assay of maximin H5 isoforms

The antimicrobial activity of MH5N was tested and exhibited activity against *S. aureus* (MIC = 90 μM) but was found to be ineffective against *E. coli*, which is consistent with previous reports [30]. In contrast, MH5C was found to have a reduced capability to inactivate *S. aureus* (MIC = 180 μM) but was effective against *E. coli* (MIC = 180 μM). The antibacterial activity of both peptides is comparable with that of other anionic AMPs [1,16] such as *Cn*-AMP2 and *Cn*-AMP3 from the plant, *Cocos nucifera* [40], and GH-1_L, and GH-1_D, from the toad, *Bombina orientalis* [41].

3.2. The haemolytic ability of maximin H5 isoforms

The ability of MH5N and MH5C to interact with human erythrocytes was assayed and it was found that below concentrations of 25 μM, both peptides showed low, comparable haemolytic activity, which was <12%. Above 25 μM, MH5N became progressively more haemolytic than MH5C although both peptides remained moderately active towards erythrocytes, inducing between circa 15% and 25% lysis at peptide concentrations above 450 μM (Fig. 1). These data also showed that at its MIC for *S. aureus* (90 μM) MH5N exhibited haemolysis levels of 20% whilst at its MIC for both *S. aureus* and *E. coli* (180 μM) MH5C induced haemolysis levels of 12%.

3.3. Secondary structural analysis of maximin H5 isoforms

The conformational behaviour of MH5N and MH5C in different environments was investigated using CD spectroscopy. In aqueous solution, both peptides were not well folded with a maximum at 212 nm and a

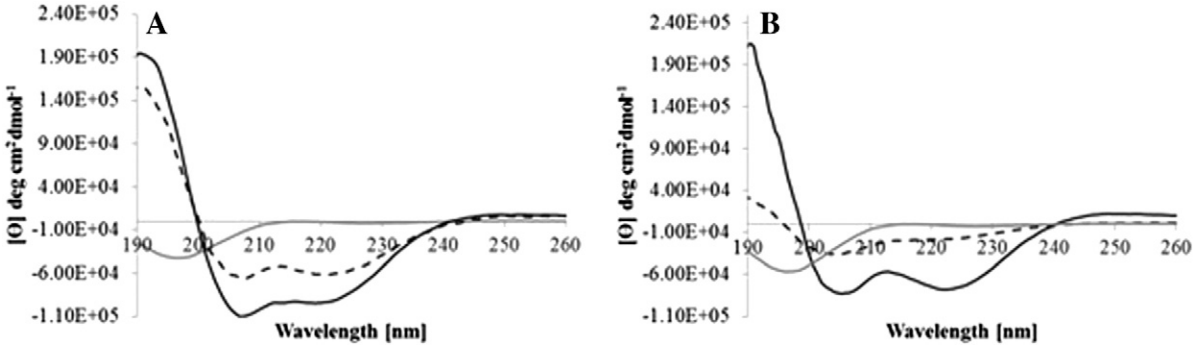

Fig. 2. CD structural analysis of maximin H5 isoforms in solvent systems. The figure shows CD spectra for MH5N (A) and MH5C (B) in the presence of PBS (grey); TFE/water (50% v/v) (black) and DMPC (dotted black). Analysis of these spectra indicated that in PBS, both peptides were not well folded with a maximum at 212 nm and a minimum at 195 nm, which is characteristic of random coil and β-sheet structure. For both MH5C and MH5N, their α-helical content was <10% (Supplementary data, Table 1). In the presence of TFE/water (50% v/v), both peptides displayed a curve characterised by a double minimum at 205 and 225 nm, which is typical of α-helical peptides. Analysis of these spectra showed that MH5C and MH5N possessed α-helical contents of >60% with the remaining structural contributions to their molecular architecture coming from random coil and β-type structures (Supplementary data, Table 1). Similarly, in the presence of DMPC, analysis of these spectra showed that α-helical contributions to the structures of MH5N and MH5C were 42% and 16% respectively.

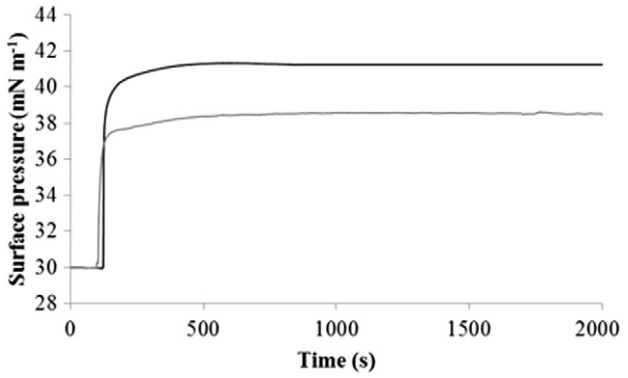

Fig. 3. The interaction of maximin H5 isoforms with lipid monolayers. The figure shows the interaction of MH5N (black) and MH5C (grey) with monolayers formed from DMPC. MH5N showed a greater ability to partition into these monolayers than MH5C with these peptides inducing maximal surface pressure changes of 10.8 mN m^{-1} and 7.8 mN m^{-1}, respectively.

minimum at 195 nm (Fig. 2). Analysis of these CD spectra showed that MH5N and MH5C both possessed <10% α-helical structure and were predominantly formed from random coil and β-type structures (Supplementary data, Table 1). A key step in the membrane interaction of AMPs involves the adoption of secondary structures in the anisotropic environment of the interface [29], which is often investigated using TFE, a lipophilic, membrane-mimicking solvent [42]. Fig. 2 shows that in a TFE/water mixture (50% v/v), both MH5N and MH5C display a curve, which is characterised by a double minimum at 205 and 225 nm and typical of α-helical peptides. Further analysis of these CD spectra showed that both peptides were >60% α-helical with the remaining structural contributions to these peptides coming from random coil and β-type architectures (Supplementary data, Table 1). The outer leaflets of erythrocyte plasma membranes are composed mainly of choline lipids, predominantly phosphatidylcholine (PC), which was used in the present study as a lipid model for erythrocyte membranes [43]. The conformational preferences of MH5N and MH5C in the presence of DMPC were investigated: the resulting spectra for both peptides showed negative bands around 222 and 210 nm, indicative of the presence of α-helical structure (Fig. 2). Analysis of these CD spectra showed that the α-helical contributions to the structure of MH5N were 42% whilst those for MH5C were 16%. For both peptides, the remaining contributions to their molecular architecture came from random coil and β-type structures (Supplementary data, Table 1).

3.4. Lipid monolayer analysis and the lytic ability of maximin H5 isoforms

The interaction of maximin H5 isoforms with membranes was investigated using monolayers formed from DMPC. Both peptides interacted rapidly with these monolayers, inducing maximal surface pressure changes of 7.8 mN m^{-1} and 10.8 mN m^{-1} for MH5C and MH5N respectively (Fig. 3). These surface pressure changes indicate high levels of lipid interaction, which are consistent with disruption of the monolayer acyl chain region by maximin H5 and imply a major role for hydrophobic forces in driving the membrane interactions of the peptide. The interaction of maximin H5 isoforms with membranes was further investigated using large unilamellar vesicles (LUVs) formed from DMPC and containing calcein. Both peptides were found to possess membranolytic ability that paralleled their interactions with lipid monolayers: MH5N and MH5C induced 64% and 55% lysis of these LUVs respectively.

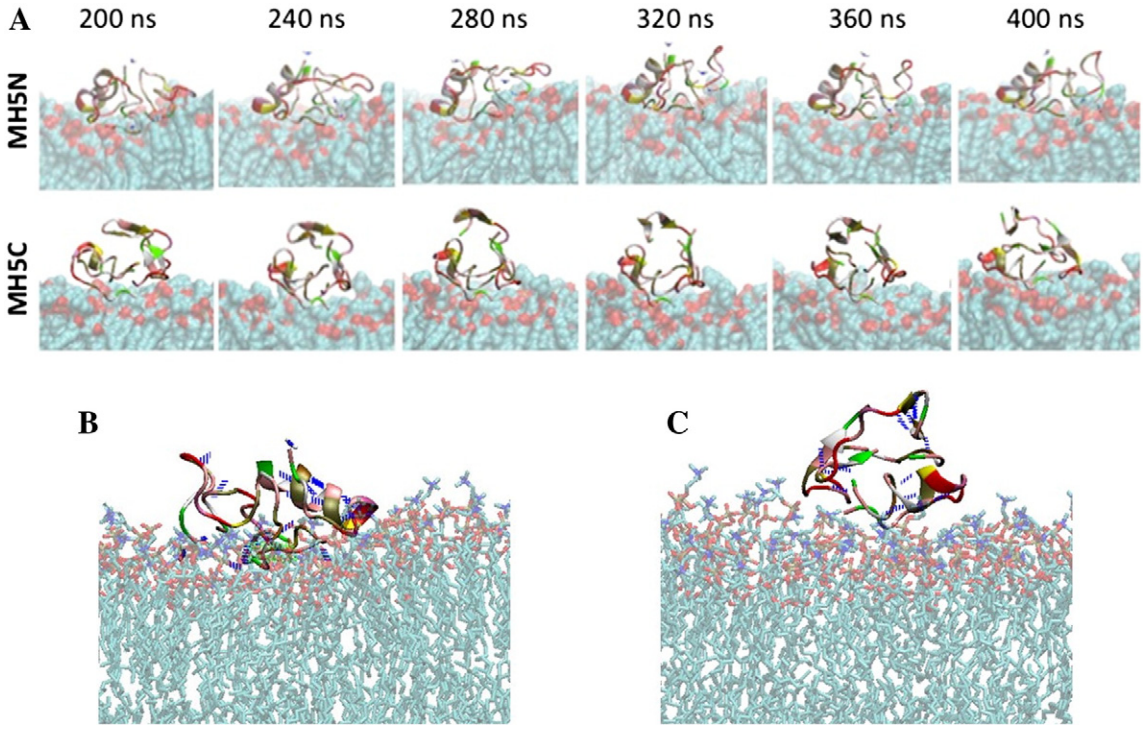

Fig. 4. MD simulations of the membrane interaction of maximin H5 isoforms. The figure shows MD simulations for the interaction of MH5C and MH5N with membranes formed from DMPC. In these simulations, three molecules of each peptide were initially orientated parallel to the bilayer and upon interaction with the bilayer surface, each group of three peptides formed an aggregate and partitioned into the membrane. Each aggregate showed a series of changes in its overall levels of secondary structure up to 200 ns but thereafter showed only very minor changes in this structure up to 400 ns (A). Snapshots of the aggregates formed by these peptides after 400 ns showed that MH5N penetrated DMPC membranes more deeply than MH5C (A and B). These figures also showed that the aggregates formed by MH5N and MH5C respectively were stabilised by intra-peptide and inter peptide hydrogen bonds (specific examples shown in Figs. 6 and 7). MH5C formed no hydrogen bonds with DMPC lipids (C) but in contrast, MH5N formed multiple hydrogen bonds with these lipids (specific examples shown in Fig. 6). However, the C-terminal amide moiety of MH5N appeared to form no hydrogen bonds with DMPC lipids.

3.5. Molecular dynamic simulations of maximin H5 isoforms

Molecular dynamic (MD) simulations were used to model and characterise the interaction of MH5C and MH5N with membranes formed from DMPC to provide insight into the mechanism of membrane partitioning utilised by maximin H5 (Figs. 4–6). In these simulations, three molecules of each peptide were initially orientated parallel to the bilayer and in each case, after 20 ns, these three molecules interacted with each other prior to interaction at the bilayer surface. Upon interaction with the bilayer surface, each group of three peptides formed an aggregate. This showed a series of changes in its overall levels of secondary structure up to 200 ns but thereafter showed only very minor changes in this structure up to 400 ns (Fig. 4A). Analysis of snapshots of the aggregates formed by MH5C and MH5N after 400 ns (Fig. 4A, B and C) predicted that the secondary structure elements adopted by these peptides in the presence of DMPC (Fig. 5A and B) were generally consistent with those determined by CD spectroscopy (Supplementary material Table 1). In the case of MH5N, two peptides were predicted to predominantly form unfolded, or β-type structures, but the third was predicted to possess overall levels of α-helicity of circa 40%. This α-helical structure was localised within an N-terminal segment comprising residues I1–S10 of the peptide, and a short C-terminal region comprising residues V16–L(NH_2)20 (Fig. 4A and B). In the case of MH5C, two peptide molecules were also predicted to mainly form unfolded, or β-type structures, but in contrast to MH5N, the third peptide of MH5C was predicted to possess levels of α-helical structure that accounted for only circa 15% of the peptide's overall structure. This α-helical structure predominantly lay in an N-terminal segment, residues I1–V5, and a C-terminal region, residues V16–L20 (Fig. 5A and B).

Partial density profiles were derived from MD simulations and predicted that aggregates of MH5C and MH5N respectively (Fig. 5C and D) would penetrate the hydrophobic core region of DMPC membranes. However, aggregates of MH5N (Fig. 5C) showed deeper levels of membrane penetration levels than those of the MH5C (Fig. 5D). Snapshots of the aggregates formed by MH5C and MH5N after 400 ns were further analysed and showed that the penetration of DMPC membranes by these aggregates involved a variety of intra-peptide, inter-peptide and peptide–lipid hydrogen bonds although via clearly different mechanisms (Figs. 4–6). A major difference between these mechanisms was that MH5C showed no peptide–lipid hydrogen bonds in its interaction with DMPC membranes whereas MH5N formed multiple hydrogen bonds with lipid head-groups (Fig. 6). For example, the L8 residue of one unfolded MH5N peptide formed a hydrogen bond with the phosphate group of a DMPC lipid whilst the I1 residue of the second unfolded MH5N peptide formed hydrogen bonds with the phosphate group of another two DMPC lipids (Fig. 6). The L(NH_2)20 groups of all three MH5N peptides lay

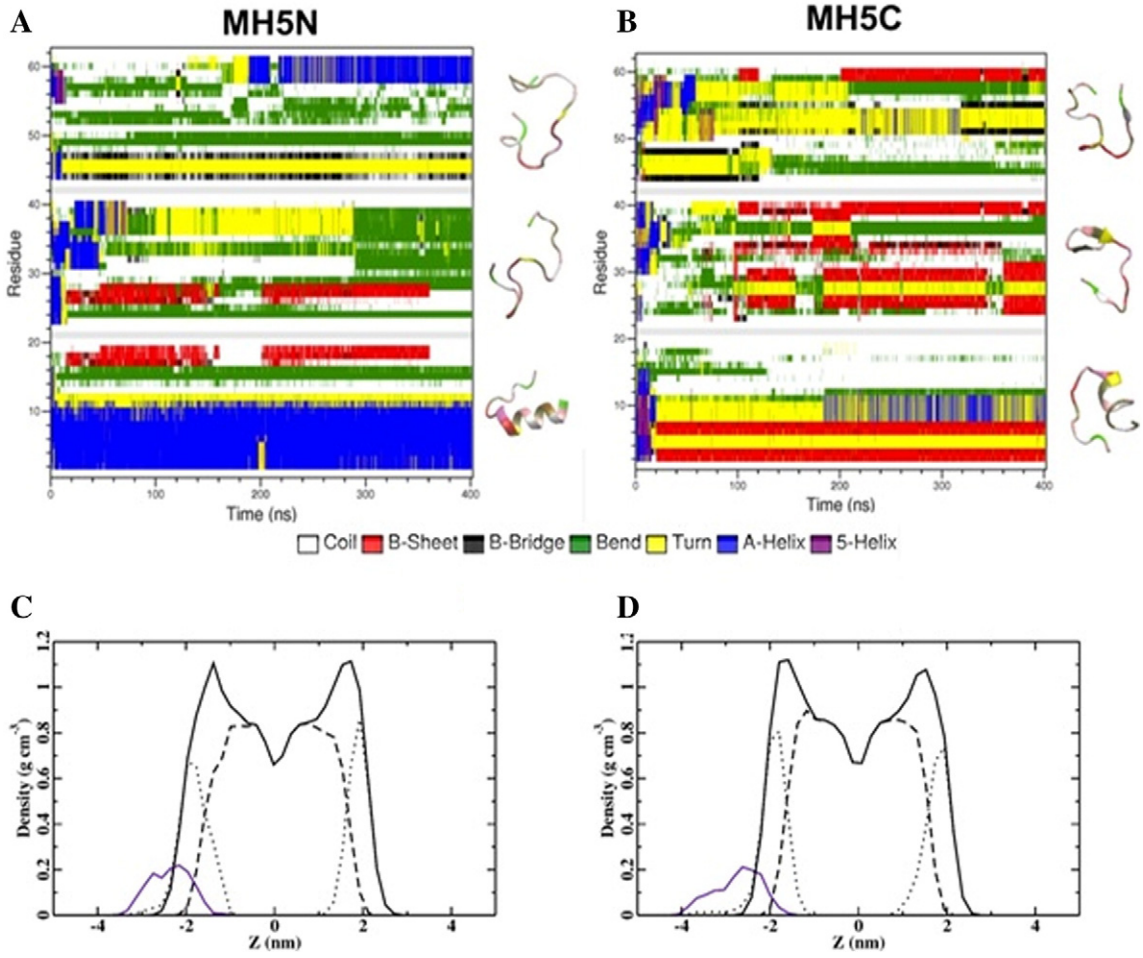

Fig. 5. MD predictions for the secondary structures of maximin H5 isoforms. Panels A and B show the secondary structure elements predicted for MH5N and MH5C by MD simulations. MH5N and MH5C showed levels of α-helicity that were circa 40% and 15% (in blue), respectively, which is generally consistent with those determined by CD spectroscopy. Partial density profiles were also generated by these MD simulations (C and D) and the graphic in each panel shows partial densities of the components in these peptide–lipid systems: overall lipid density (solid black line), lipid head-groups (dots), lipid tails groups (dashed line) and peptide (purple line). Essentially, these partial density profiles predicted that MH5N (C) would penetrate the hydrophobic membrane core region of DMPC membranes more deeply than MH5C (D).

near the membrane surface but did not form hydrogen bonds with DMPC lipids (Figs. 4 and 5).

A second major difference between the interaction of MH5C and MH5N with DMPC membranes lay in the role of the α-helical peptide present in the aggregates of both peptides. Snapshots of the aggregates formed by MH5N after 400 ns showed that its α-helical peptide penetrated the bilayer at an angle of circa 45° in a hairpin-type structure (Fig. 4A and B). One arm of this structure was formed by the N-terminal residues, I1–S10, in a strongly α-helical conformation, whilst the other arm comprised a disordered region, which was terminated by a short α-helical segment at the C-terminus of the peptide formed by residues L16–L(NH_2)20. This oblique orientation of MH5N was stabilised by hydrogen bonds between residues in the two α-helical regions of the peptide and phosphate groups in the lipid's head-group region (Fig. 4A and B). Complementing these peptide–lipid interactions was an intra-peptide hydrogen bond between the C-terminal residue, L(NH_2)20, of MH5N and its N-terminal residue, I1 (Fig. 7). The corresponding snapshots of MH5C showed that the peptide penetrated DMPC membranes in an orientation and structural conformation that resembled that observed for MH5N (Fig. 4A and C). However, in contrast to MH5N, the α-helical arm of the MH5C hairpin was truncated and comprised residues, I1–V5, with the result that the disordered region of the juxtaposed arm was elongated before termination by a C-terminal, α-helical segment formed by residues V16–L20. This oblique orientation of MH5C was primarily stabilised by hydrogen bonds between residues in the two α-helical regions of the peptide and phosphate groups in the lipid's head-group region (Fig. 4A and C). However, in further contrast to MH5N, L20 of MH5C was found to be distal from the N-terminal residue, I1, of the peptide with no evidence of hydrogen bonding between these two residues (Fig. 7).

4. Discussion

Maximin H5 is an anionic antibacterial peptide recently identified in the brains and skin secretions of the Australian toad, *B. maxima* and it has a narrow spectrum of antimicrobial activity having been reported to kill only *S. aureus* [26,27,30]. These observations give maximin H5 potential interest as a drug for development in the fight against methicillin-resistant *S. aureus* (MRSA), which is currently a major global cause of nosocomial and other infections [44]. However, for successful therapeutic application, the toxicity of the peptide towards human cells must be characterised and currently, no major investigations into this area appear to have been undertaken. Accordingly, here, we have investigated the activity of maximin H5 against bacteria and human erythrocytes and determined the role of C-terminal amidation in this activity.

Native maximin H5 showed no action against *E. coli*, confirming previous reports [30]. However, when modified by C-terminal deamination, the peptide exhibited activity against this organism (MIC = 180 μM). This result clearly demonstrates that the resistance of *E. coli* to the action of maximin H5 depends upon the presence of the peptide's C-terminal amide moiety and strongly supports recent work [39]. Using MD simulations, these latter authors predicted that H-bonding between the C-terminal amide group of maximin H5 and a lipid receptor in *E. coli* membranes helped immobilise the peptide on the membrane surface, thereby effectively rendering the organism resistant to the action of maximin H5 [39]. C-terminally deaminated maximin H5 differs from the native peptide in its ability to inactivate *S. aureus*, exhibiting reduced toxicity towards the organism (MIC = 180 μM) as compared to that of maximin H5 (MIC of 90 μM). This clearly suggests that the peptide's C-terminal amide group is required for efficient activity against the organism. Indeed, given that this C-terminal amide group, along with its N-terminal counterpart, are the only positively charged moieties possessed by maximin H5, a likely role for both these amide groups might be to assist in targeting anionic components of the membranes possessed by *S. aureus* [30]. A similar targeting function would seem ascribable to the C-terminal amide moiety possessed by a number of isoforms of the peptide, which also lack cationic residues and have been identified as potent antibacterial agents that function in the brain of *B. maxima* [26]. It is perhaps worthy of note

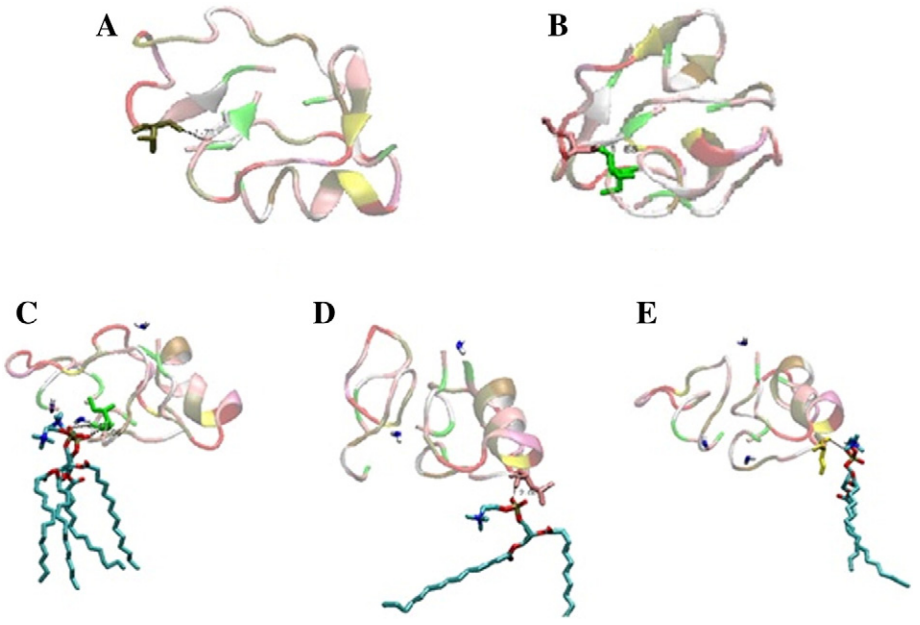

Fig. 6. The peptide–peptide and peptide–lipid interactions of maximin H5 isoforms. Aggregates of both MH5C and MH5N were found to form intra-peptide (Fig. 7) and inter peptide hydrogen bonds (A–E). As examples, the V16 residue of one unfolded peptide formed a hydrogen bond with G18 of the other unfolded peptide in MH5C aggregates (A). In the case of MH5N, the I1 residue of one unfolded peptide hydrogen bonded to the I1 residue of the other unfolded peptide in these aggregates (B). MH5C formed no hydrogen bonds with DMPC lipids (Fig. 4C) but in contrast, MH5N formed multiple hydrogen bonds with these lipids (C–E). For example, the I1 residue of an unfolded peptide in MH5N aggregates formed hydrogen bonds with the phosphate group of two DMPC lipids (C). The other unfolded peptide in these aggregates hydrogen bonded to the phosphate group of two DMPC lipids via its L8 residue (D) and its S10 residue (E).

that a number of these latter AMPs were also found to possess antinoceptive function [26], suggesting that maximin H5 and its isoforms may serve as neuropeptides and it is well established that C-terminal amidation is essential for the function of many of these neuronal signalling molecules [45].

Native maximin H5 was found to possess moderate haemolytic activity (generally below 25%; Fig. 1) that was reduced by up to 12% on C-terminal deamination of the peptide (Fig. 1). Reinforcing these results, native maximin H5 induced dye release of 64% from DMPC vesicles, which were taken as model erythrocyte membranes, however, dye release by the peptide was decreased to 55% in the case of the C-terminally deaminated peptide. In combination, these results clearly suggest a role for the C-terminal amide group of maximin H5 in the mechanism facilitating the peptide's haemolytic activity. Investigation into the mechanism underpinning the haemolytic activity of native maximin H5 suggested that the peptide was able to self-associate and penetrate erythrocyte membranes via the formation of an aggregate structure (Fig. 4A and B). This aggregate associated with the membrane via a variety of peptide–lipid hydrogen bonding interactions, which, however, did not involve the C-terminal amide, L(NH_2), groups of the contributing maximin H5 peptides (Figs. 4B and 7A). Two of the peptides forming these aggregates were unfolded and appeared to play a minor role in the membrane interactions of native maximin H5 by stabilising the bilayer penetration of the remaining peptide contributing to the aggregate (Fig. 4A and B). The latter peptide appeared to be primarily responsible for membrane penetration by maximin H5 and adopted a lipid interactive, hairpin-type conformation whose bilayer partitioning was stabilised by a variety of lipid–peptide and intra peptide bonds (Figs. 4A, B, 6 and 7A). The net negative charge carried by maximin H5 results from an internal cluster of D residues, which were distal from the membrane surface and appeared to play no direct role in the membrane interactions of the peptide (Figs. 4B and 7A). Similar observations have previously been reported and it has been suggested that these residues primarily serve a structural role [39]. The C-terminal amide group of maximin H5, L(NH_2), hydrogen bonded to the N-terminal residue of the peptide, I1, which terminated the major arm of the hairpin structure adopted by maximin H5 (Fig. 7A and C). Formed by residues, I1–S10, this sequence adopted an α-helical structure, which induced deep insertion of native maximin H5 into membranes at an angle of circa 40° (Figs. 4B, 5C and 7A). It has previously been shown that residues, I1–S10 form a tilted peptide [46,47], which is an α-helix with an increasingly asymmetric distribution of hydrophobicity along the α-helical long axis that induces membrane penetration at a shallow angle between 30° and 60° [48,49]. However, our investigations also showed that the C-terminal deamination of maximin H5 removed the ability of its I1 and L20 residues to hydrogen bond with each other and caused these residues to move apart from a separation of 4.5 Å to 9.95 Å (Fig. 7), These actions led to lower levels of N-terminal tilted structure in the peptide and a decreased ability to penetrate membranes (Figs. 4B, 5D and 7B). Taken in combination, these observations clearly suggest that a major function of the C-terminal amide group of maximin H5 is to stabilise the levels of membrane interactive, oblique orientated α-helical structure adopted by the peptide in its haemolytic activity. These observations would also seem to suggest that hydrophobicity driven interactions make a major contribution to the ability of native maximin H5 to penetrate membranes and in this sense, although anionic, the peptide resembles many cationic AMPs [46,47].

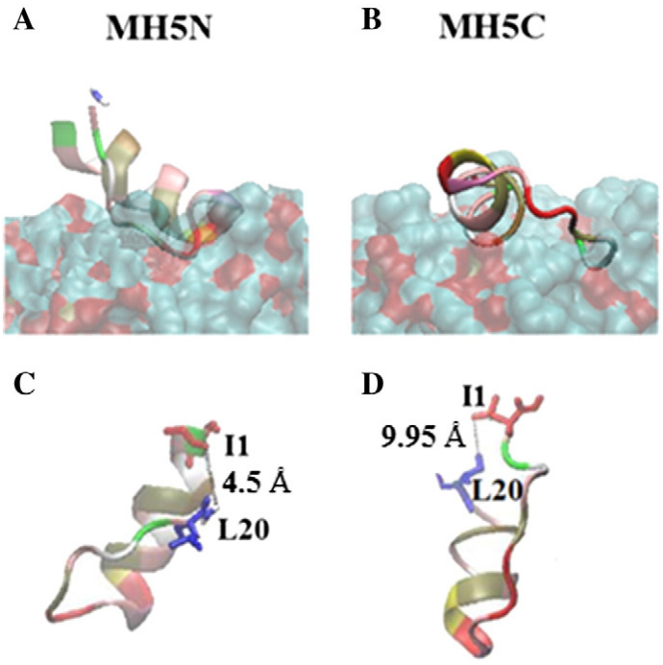

Fig. 7. C-terminal intra-peptide hydrogen bonding by maximin H5 isoforms. Panels A and B show MD predictions for the secondary structure of MH5N and MH5C when interacting with DMPC membranes, which for clarity are shown in panels C and D with the lipids removed. These simulations predicted that MH5N would penetrate these membranes at an angle of circa 45° in a hairpin-type structure (A). One arm of this structure was formed by the N-terminal residues, I1–S10, in a strongly α-helical conformation, whilst the other arm comprised a disordered region, which was terminated by a short α-helical segment at the C-terminus of the peptide formed by residue L16–L(NH_2)20. This overall conformation of MH5N was stabilised by a hydrogen bond 4 between its C-terminal residue, L(NH_2)20, and its N-terminal residue, I1 (4.5 Å, C). Corresponding modelling for MH5C predicted that the peptide would penetrate the bilayer in an orientation and structural conformation that resembled that observed for MH5N (B). However, in contrast to MH5N, the α-helical arm of the MH5C hairpin was truncated and comprised residues, L1–V5, with the result that the disordered region of the juxtaposed arm was elongated before termination by a C-terminal, α-helical segment formed by residue V16–L20 (D). In further contrast to MH5N, L20 of MH5C was found to be distal from the N-terminal residue, I1, of the peptide with no evidence of H-bonding between these two residues (9.95 Å, D).

In summary, the data presented here suggest that the haemolytic ability of native maximin H5 may render it a poor candidate for therapeutic development. For example, the level of haemolysis was 20% at concentrations of the peptide required to inactivate *S. aureus* (Fig. 1). However, when maximin H5 was C-terminally deaminated, although the toxicity of the peptide to the latter organism was reduced, its range of target bacteria was broadened. Also its haemolytic activity were significantly decreased, typically 12% at concentrations of the peptide found to inactivate both *S. aureus* and *E. coli* (Fig. 1). Consistent with previous reports [50], these data show that the antimicrobial efficacy and specificity of maximin H5 can be attenuated by sequence modification and may assist in the development of variants of the peptide with the potential to serve as anti-infectives. The data presented here also suggests that the C-terminal amide moiety may play a role in the antimicrobial and cytotoxic activity of maximin H5 by the stabilisation of membrane interactive, tilted peptide structure. Indeed, the data presented here confirm recent theoretical predictions for maximin H5 [46,47] and add it to the growing number of AMPs that utilise tilted peptide structure to facilitate their membrane interactions [3].

Supplementary data to this article can be found online at http://dx.doi.org/10.1016/j.bbamem.2015.01.014.

Conflict of interest

The authors declare that there are no conflicts of interest.

Acknowledgements

The authors thank HPCT at the University of Central Lancashire. The authors also thank Kamal Badiani and Pinki Badiani from Pepceuticals Ltd.

References

[1] F. Harris, S.R. Dennison, D.A. Phoenix, Anionic antimicrobial peptides from eukaryotic organisms, Curr. Protein Pept. Sci. 10 (2009) 585–606.
[2] D.A. Phoenix, S.R. Dennison, F. Harris, Cationic antimicrobial peptides, Antimicrobial Peptides, Wiley-VCH Verlag GmbH & Co. KGaA, 2013, pp. 39–81.
[3] D.A. Phoenix, S.R. Dennison, F. Harris, Models for the membrane interactions of antimicrobial peptides, in: D.A. Phoenix, S.R. Dennison, F. Harris (Eds.), Antimicrobial Peptides, Wiley, Germany, 2013, pp. 145–180.
[4] S.R. Dennison, J. Wallace, F. Harris, D.A. Phoenix, Amphiphilic alpha-helical antimicrobial peptides and their structure/function relationships, Protein Pept. Lett. 12 (2005) 31–39.
[5] D. Andreu, L. Rivas, Animal antimicrobial peptides: an overview, Biopolymers 47 (1998) 415–433.
[6] G.S. Wang, Post-translational modifications of natural antimicrobial peptides and strategies for peptide engineering, Curr. Biotechnol. 1 (2012) 72–79.
[7] A.J. Otero-González, B.S. Magalhães, M. Garcia-Villarino, C. López-Abarrategui, D.A. Sousa, S.C. Dias, O.L. Franco, Antimicrobial peptides from marine invertebrates as a new frontier for microbial infection control, FASEB J. 24 (2010) 1320–1334.
[8] M.I. El-Gamal, M.S. Abdel-Maksoud, C.H. Oh, Recent advances in the research and development of marine antimicrobial peptides, Curr. Top. Med. Chem. 13 (2013) 2026–2033.
[9] V.L.T. Hoang, S.-K. Kim, Antimicrobial peptides from marine sources, Curr. Protein Pept. Sci. 14 (2013) 205–211.
[10] F. Harris, S. Dennison, D. Phoenix, Anionic antimicrobial peptides from eukaryotic organisms and their mechanisms of action, Curr. Chem. Biol. 5 (2011) 142–153.
[11] A. Jilek, G. Kreil, D-Amino acids in animal peptides, Monatsh. Chem. 139 (2008) 1–5.
[12] M. Simmaco, G. Kreil, D. Barra, Bombinins, antimicrobial peptides from *Bombina* species, Biochim. Biophys. Acta 1788 (2009) 1551–1555.
[13] J.M.S. Koh, P.S. Bansal, A.M. Torres, P.W. Kuchel, Platypus venom: source of novel compounds, Aust. J. Zool. 57 (2009) 203–210.
[14] H. El Hajjaji, J.-F. Collet, Disulfide bond formation, Post-translational Modification of Protein Biopharmaceuticals, Wiley-VCH Verlag GmbH & Co. KGaA, 2009, pp. 277–294.
[15] R. Condé, M. Argüello, J. Izquierdo, R.I. Noguez, M. Moreno, H. Lanz, Natural antimicrobial peptides from eukaryotic organismsAvailable from: http://www.intechopen.com/books/antimicrobial-agents/natural-antimicrobial-peptides-from-eukaryotic-organisms in: V. Bobbarala (Ed.), Antimicrobial Agents, InTech, 2012.
[16] S. Prabhu, S. Dennison, B. Lea, T. Snape, I. Nicholl, I. Radek, F. Harris, Anionic antimicrobial and anticancer peptides from plants, Crit. Rev. Plant Sci. 32 (2013) 303–320.
[17] R. Burman, S. Gunasekera, A.A. Strömstedt, U. Göransson, Chemistry and biology of cyclotides: circular plant peptides outside the box, J. Nat. Prod. 77 (2014) 724–736.
[18] S.T. Henriques, Phosphatidylethanolamine-binding is a conserved feature of cyclotide–membrane interactions, J. Biol. Chem. 287 (2012) 33629–33643.
[19] S.T. Henriques, Y.-H. Huang, K.J. Rosengren, H.G. Franquelim, F.A. Carvalho, A. Johnson, S. Sonza, G. Tachedjian, M.A.R.B. Castanho, N.L. Daly, D.J. Craik, Decoding the membrane activity of the cyclotide kalata B1: the importance of phosphatidylethanolamine phospholipids and lipid organization on hemolytic and anti-HIV activities, J. Biol. Chem. 286 (2011) 24231–24241.
[20] M.H. Cardoso, N.B. Cobacho, M.D. Cherobim, M.F.C. Pinto, C.e.a. Santos, Insights into the antimicrobial activities of unusual antimicrobial peptide families from amphibian skin, J. Clin. Toxicol. 4 (2014) 1–10.
[21] N.M. Mehta, S.E. Carpenter, A.P. Consalvo, C-terminal α-amidation, Post-translational Modification of Protein Biopharmaceuticals, Wiley-VCH Verlag GmbH & Co. KGaA, 2009, pp. 253–276.
[22] J.M. Conlon, J. Kolodziejek, N. Nowotny, Antimicrobial peptides from the skins of North American frogs, Biochim. Biophys. Acta 1788 (2009) 1556–1563.
[23] E.F. Haney, H.N. Hunter, K. Matsuzaki, H.J. Vogel, Solution NMR studies of amphibian antimicrobial peptides: linking structure to function? Biochim. Biophys. Acta 1788 (2009) 1639–1655.
[24] H.S. Won, S.-J. Kang, B.-J. Lee, Action mechanism and structural requirements of the antimicrobial peptides, gaegurins, Biochim. Biophys. Acta 1788 (2009) 1620–1629.
[25] S.R. Dennison, F. Harris, T. Bhatt, J. Singh, D.A. Phoenix, The effect of C-terminal amidation on the efficacy and selectivity of antimicrobial and anticancer peptides, Mol. Cell. Biochem. 332 (2009) 43–50.
[26] R. Liu, H. Liu, Y. Ma, J. Wu, H. Yang, H. Ye, R. Lai, There are abundant antimicrobial peptides in brains of two kinds of *Bombina* toads, J. Proteome Res. 10 (2011) 1806–1815.
[27] W.-H. Lee, Y. Li, R. Lai, S. Li, Y. Zhang, W. Wang, Variety of antimicrobial peptides in the *Bombina maxima* toad and evidence of their rapid diversification, Eur. J. Immunol. 35 (2005) 1220–1229.
[28] R. Lai, Y.-T. Zheng, J.-H. Shen, G.-J. Liu, H. Liu, W.-H. Lee, S.-Z. Tang, Y. Zhang, Antimicrobial peptides from skin secretions of Chinese red belly toad *Bombina maxima*, Peptides 23 (2002) 427–435.
[29] S.R. Dennison, D.A. Phoenix, Influence of C-terminal amidation on the efficacy of modelin-5, Biochemistry 50 (2011) 1514–1523.
[30] R. Lai, H. Liu, W.H. Lee, Y. Zhang, An anionic antimicrobial peptide from toad *Bombina maxima*, Biochem. Biophys. Res. Commun. 295 (2002) 796–799.
[31] S.R. Dennison, L.H. Morton, D.A. Phoenix, Role of molecular architecture on the relative efficacy of aurein 2.5 and modelin 5, Biochim. Biophys. Acta 1818 (2012) 2094–2102.
[32] D. Oh, S.Y. Shin, S. Lee, J.H. Kang, S.D. Kim, P.D. Ryu, K.S. Hahm, Y. Kim, Role of the hinge region and the tryptophan residue in the synthetic antimicrobial peptides, cecropin A(1–8)-magainin 2(1–12) and its analogues, on their antibiotic activities and structures, Biochemistry 39 (2000) 11855–11864.
[33] Y.M. Song, Y. Park, S.S. Lim, S.T. Yang, E.R. Woo, I.S. Park, J.S. Lee, J.I. Kim, K.S. Hahm, Y. Kim, S.Y. Shin, Cell selectivity and mechanism of action of antimicrobial model peptides containing peptoid residues, Biochemistry 44 (2005) 12094–12106.
[34] N.J. Greenfield, Using circular dichroism spectra to estimate protein secondary structure, Nat. Prot. 6 (2006) 2876–2890.
[35] L. Whitmore, B. Woollett, A.J. Miles, R.W. Janes, B.A. Wallace, The protein circular dichroism data bank, a Web-based site for access to circular dichroism spectroscopic data, Structure 18 (2010) 1267–1269.
[36] L. Whitmore, B.A. Wallace, Protein secondary structure analyses from circular dichroism spectroscopy: methods and reference databases, Biopolymers 89 (2008) 392–400.
[37] L. Whitmore, B.A. Wallace, DICHROWEB, an online server for protein secondary structure analyses from circular dichroism spectroscopic data, Nucleic Acids Res. 32 (2004) W668–W673.
[38] A. Seeling, Local anesthetics and pressure: a comparison of dibucaine binding to lipid monolayers and bilayers, Biochim. Biophys. Acta 899 (1987) 196–204.
[39] S.R. Dennison, F. Harris, M. Mura, L.H.G. Morton, A. Zvelindovsky, D.A. Phoenix, A novel form of bacterial resistance to the action of eukaryotic host defense peptides, the use of a lipid receptor, Biochemistry 52 (2013) 6021–6029.
[40] S.M. Mandal, S. Dey, M. Mandal, S. Sarkar, S. Maria-Neto, O.L. Franco, Identification and structural insights of three novel antimicrobial peptides isolated from green coconut water, Peptides 30 (2009) 633–637.
[41] M.L. Mangoni, N. Grovale, A. Giorgi, G. Mignogna, M. Simmaco, D. Barra, Structure–function relationships in bombinins H, antimicrobial peptides from *Bombina* skin secretions, Peptides 21 (2000) 1673–1679.
[42] P.Z. Luo, R.L. Baldwin, Mechanism of helix induction by trifluoroethanol: a framework for extrapolating the helix-forming properties of peptides from trifluoroethanol/water mixtures back to water, Biochemistry 36 (1997) 8413–8421.
[43] J.A. Virtanen, K.H. Cheng, P. Somerharju, Phospholipid composition of the mammalian red cell membrane can be rationalized by a superlattice model, PNAS 95 (1998) 4964–4969.
[44] H. Patel, Y. Vaghasiya, B.R.M. Vyas, S. Chanda, Emergence of methicillin-resistant *Staphylococcus aureus* (MRSA) as a public-health threat and future directions of antibiotic therapy for MRSA infections, Anti Infect. Agents 10 (2012) 149–157.
[45] K.-H. Kim, B.L. Seong, Peptide amidation: production of peptide hormones in vivo and in vitro, Biotechnol. Bioprocess Eng. 6 (2001) 244–251.
[46] S.R. Dennison, F. Harris, D.A. Phoenix, Are oblique orientated alpha-helices used by antimicrobial peptides for membrane invasion? Protein Pept. Lett. 12 (2005) 27–29.
[47] D.A. Phoenix, S.R. Dennison, F. Harris, Graphical techniques to visualize the amphiphilic structures of antimicrobial peptides, Antimicrobial Peptides, Wiley-VCH Verlag GmbH & Co. KGaA, 2013, pp. 115–144.
[48] F. Harris, S. Dennison, D.A. Phoenix, The prediction of hydrophobicity gradients within membrane interactive protein alpha-helices using a novel graphical technique, Protein Pept. Lett. 13 (2006) 595–600.
[49] F. Harris, A. Daman, J. Wallace, S.R. Dennison, D.A. Phoenix, Oblique orientated alpha-helices and their prediction, Curr. Protein Pept. Sci. 7 (2006) 529–537.
[50] G.S. Wang, K.M. Watson, A. Peterkofsky, R.W. Buckheit, Identification of novel human immunodeficiency virus type 1-inhibitory peptides based on the antimicrobial peptide database, Antimicrob. Agents Chemother. 54 (2010) 1343–1346.